Helical Twisting Power of Three-ring Chiral Molecules and Polymerization in Cholesteric Electrolyte Solutions

Hitoshi Hayashi,[1,2] Aohan Wang,[2] Kohsuke Kawabata,[2] Hiromasa Goto[2,*]

[1]*Advanced Research, Research Laboratories, DENSO CORPORATION, 500-1, Minamiyama, Komenoki-cho, Nisshin, Aichi 470-0111, Japan.*

[2]*Division of Materials Science, Faculty of Pure and Applied Sciences, University of Tsukuba, Tsukuba, Ibaraki 305-8573, Japan*

Corresponding to H. Goto, e-mail: gotoh@ims.tsukuba.ac.jp

Highlights

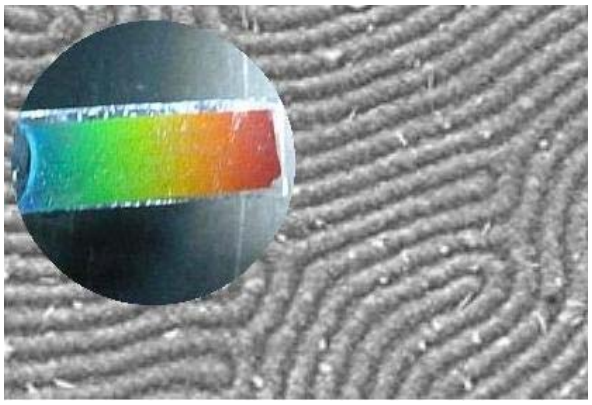

·Three-ring type chiral compounds functioned as chiral inducers.
·Polymerization in the cholesteric liquid crystal produced optically active polymers.
· Helicity of the polymers depends on helical twisting power of the chiral inducers.
· Chiroptical activity of the polymer could be tuned by electrochemical method.

Helical Twisting Power of Three-ring Chiral Molecules and Polymerization in Cholesteric Electrolyte Solutions

Hitoshi Hayashi,[1,2] Aohan Wang,[2] Kohsuke Kawabata,[2] Hiromasa Goto[2,*]

[1]Advanced Research, Research Laboratories, DENSO CORPORATION, 500-1, Minamiyama, Komenoki-cho, Nisshin, Aichi 470-0111, Japan.

[2] Division of Materials Science, Faculty of Pure and Applied Sciences, University of Tsukuba, Tsukuba, Ibaraki 305-8573, Japan

Corresponding to H. Goto, e-mail: gotoh@ims.tsukuba.ac.jp

Abstract A series of chiral three-ring type compounds with rigid shape was employed as chiral inducers for induction of chiral cholesteric liquid crystal (cholesteric LC) from achiral nematic LC. Helical twisting power of the chiral compounds was estimated with the Cano wedge method. Cholesteric LC electrolyte solution was prepared by adding the chiral compounds. Subsequently, polymerization in the cholesteric LC was carried out to produce chiroptically active polymer films. This method is different from conventional methods for synthesizing chiral polymers because neither chiral monomers nor asymmetric catalysts are employed. Surface structure and optical properties of the polymer thus prepared were examined.

Keywords; Liquid crystals, Organic compounds, Chemical synthesis, electrochemical techniques, electron microscopy, optical microscopy, nuclear magnetic resonance, electrochemical properties, microstructure, optical properties

1. Introduction

π-Conjugated polymers show electrical conductivity upon doping (addition of small amount of electron acceptor or donor). Various industrial applications, such as electrochromic devices, photovoltaics, electro-luminescent devices, organic transistors, and sensors have been investigated [1–5].

Preparation of the conjugated polymers can be performed by chemical polymerization using transition metal catalysts, oxidizers, or electrochemical polymerization. Generally, electrochemical polymerizations are conducted in isotropic liquids. The reaction provides polymers deposited on a substrate (e.g., ITO (indium-tin-oxide)-coated glass) with an epitaxial growth process. The electrochemically prepared polymer displays good redox properties and electrochemically driven change in color (electrochromism) [6–23].

Chiral π-conjugated polymers have received attention for their three-dimensional (3-D) helical structure and chiroptical activity in the visible light range because the π–π∗ transition of the main chain is in a chiral environment. Synthesis of chiral π-conjugated polymers has been carried out by chemical reactions with an asymmetric catalyst, or by preparation from chiral monomers.

Cholesteric LC is a chiral LC. Directors (molecular orientation direction expressed by a vector) are rotated progressively to form a predominantly one-handed helical structure. The helical aggregation of rod-like molecules in the liquid crystal state possesses helical periodicity, and the 3-D molecular arrangement of the LC produces structural chirality. Cholesteric LC can be employed as a chemical reaction solvent because of its fluidity and the solubility of non-LC compounds.

In previous research we have conducted polymerization in cholesteric LC with cholesterol derivatives [24]. This method is different from conventional methods for synthesizing chiral polymers because neither chiral monomers nor asymmetric catalysts are employed [25,26]. In this study we employ three-ring chiral molecules as chiral inducers (chiral dopant) instead of the cholesterol derivatives for construction of the chiral environment for asymmetric polymerization. We choose these compounds because they possess chirality with large polarization, asymmetric molecular form (molecular polarization of the ester group normal to the major axis of the molecule), and rigid shape [27–29]. The rigid molecular form provides good affinity with the nematic LC (rigid rod-like molecular shape), and the chirality can induce one-handed helical structure for the cholesteric LC. These qualities can be effective as a chiral inducer.

The three-ring chiral inducers used in this study are the series of 4-(1-(trifluoromethyl or methyl) heptyloxy carbonyl) phenyl-4'-alkoxy biphenyl-4-carboxylate (**X**HP**R**BC, **X** = TFM (trifuruoromethyl) or M (methyl), **R** = O (octyloxy) or D (decyloxy)) [30,31]. Helical twisting power of the compounds is estimated by the Cano wedge method.

A small amount of the compounds is added to 4-cyano-4'-hexyl biphenyl (6CB) as a host nematic LC, and an achiral monomer 2,5-bis[2-(3,4-ethylenedioxy) thienyl] pyridine (BEDOT-Pyr), tetrabutyl ammonium perchlorate (TBAP, electrolyte) is dissolved in the LC mixture for preparation of the cholesteric LC electrolyte solution. Here, 6CB and TBAP were obtained from Merck and Tokyo Chemical Ltd. (TCI). Next, polymerizations are performed with the electrochemical method under applied voltage. The polymers are examined with polarizing optical microscopy (POM), scanning electron microscopy (SEM), circular dichroism (CD) spectroscopy, optical rotatory dispersion (ORD), and cyclic voltammetry (CV).

The polymer films thus synthesized display fingerprint surface structure which resembles the optical texture of the cholesteric LC electrolyte solution. The films exhibit rainbow-colored appearance upon irradiation by white light. This reflected light originates from the periodic convex-concave structure of the polymer surface observable with the POM and the SEM. The films show CD and ORD. Furthermore, the polymers display redox-driven change in CD and ORD, a property derived from chiral structure produced by transcription of

the structural chirality from the cholesteric LC during polymerization. These results imply that the optically active functionality of the polymer is induced by the chiral compounds.

In this paper, we report 1) helical induction properties of a series of rigid form chiral materials, 2) synthesis of chiral polymers from achiral monomers in chiral LC, 3) comparison of the helical twisting power of the chiral compounds (for production of cholesteric LC) and helical pitch of the resultant polymer prepared in the cholesteric LC, and 4) optical properties of the polymer.

2. Experimental

2.2 Synthesis of chiral inducers

The samples employed in the present study are a series of **X**MHP**R**BC. An asymmetric center is positioned at the methyl group or trifluoromethyl group in the terminal. All samples have (*R*)-configuration at the asymmetric center, as shown in Table 1. The tree-ring type LCs were synthesized based on the previously reported method [32].

The synthetic route for TFMHPOBC (5) is shown in Scheme 1. Firstly, Compound 1 (Scheme 1) and $SOCl_2$ were mixed in dichloromethane (DCM) to introduce Cl atoms with the S_{Ni} mechanism. After refluxing the mixture for 2 hours, the chiral alcohol (2) was added to the mixture under the presence of triethylammine (NEt_3). The reaction temperature raised from 0 °C to room temperature. Subsequently, the compound thus obtained was treated with Pd-C in tetrahydrofuran (THF) solution under hydrogen flow at 0 ºC to obtain compound 3. Next, compound 3 was coupled with compound 4 after treatment of $SOCl_2$ in the presence of NEt_3 in DMF to obtain TFMHPOBC (5). Lastly, purification by column chromatography on silica gel followed by recrystallization obtained the desired product as a white solid. ^{1}H-^{13}C NMR correlation 2D-NMR (HMQC, Hetero-nuclear Multiple Quantum Coherence) of TFMHPOBC confirmed its chemical structure, as shown in Fig.1.

Mass spectroscopy measurement revealed an m/z value of the compound of 719. This value corresponds well to molecular weight of TFMHPOBC. Purity of the TFMHPOBC was 99.6% evaluated with high pressure liquid chromatography (HPLC). Purities of TFMHPDBC, MHPOBC, and MHPDBC were satisfactory (~100%). ^{19}F NMR (470 MHz, $CDCl_3$, trifluorotoluene as an internal standard) spectroscopy for TFMHPOBC confirmed that the signal of -CF_3 attached at the asymmetric center was observed at –64.0 ppm.

^{1}H-NMR for TFMHPOBC (400 MHz, $CDCl_3$ δ from TMS): 0.88 (t, 6H, *J* = 7.60 Hz), 1.29 (m, 18H), 1.88(m, 4H), 4.01 (t, 2H, *J* = 6.68 Hz), 5.55(q, 1H, *J* = 4.00 Hz),7.02 (d, 2H, *J* = 8.40 Hz), 7.36 (d, 2H, *J* = 8.40 Hz) 7.59 (d, 2H, *J* = 8.00 Hz), 7.61 (d, 2H, *J* = 8.80 Hz), 8.18 (d, 2H, *J* = 8.40 Hz), 8.23 (d, 2H, *J* = 8.40 (Hz).

^{1}H-NMR for TFMHPDBC (400 MHz, $CDCl_3$, δ from TMS): 0.88 (t, 6H, *J* = 4.60 Hz), 1.29 (m, 18H), 1.88 (m, 4H), 4.01 (t, 2H, *J* = 6.44 Hz), 5.55 (q, 1H, *J* = 4.00 Hz), 7.01 (d, 2H, *J* = 8.40 Hz), 7.36 (d, 2H, *J* =8.80 Hz) 7.61 (d, 2H, *J* =8.80 Hz), 7.71 (d, 2H, *J* = 8.80 Hz), 8.18 (d, 2H, *J* = 8.60 Hz), 8.24 (d, 2H, *J* =8.80 Hz).

^{1}H-NMR for MHPOBC (400 MHz, $CDCl_3$ δ from TMS): 0.88 (t, 6H, *J* = 5.04 Hz), 1.31(m, 21H), 1.85 (m, 4H), 4.01 (t, 2H, *J* =6.64 Hz), 5.18 (q, 1H, *J* =4.00 Hz), 7.01 (d, 2H, *J* = 8.80 Hz), 7.31 (d, 2H, *J* = 8.40 Hz) 7.61 (d, 2H, *J* = 8.80 Hz), 7.70 (d, 2H, *J* = 8.00 Hz), 8.13 (d, 2H, *J* = 8.80 Hz), 8.24 (d, 2H, *J* =8.80 Hz).

^{1}H-NMR for MHPDBC (400 MHz, $CDCl_3$ δ from TMS): 0.90 (t, 6H, *J* = 7.60 Hz), 1.29 (m, 21H), 1.82 (m, 4H), 4.01 (t, 2H, *J* = 6.64 Hz), 5.17 (q, 1H, *J* = 4.00 Hz), 7.01 (d, 2H, *J* = 8.00 Hz), 7.32 (d, 2H, *J* = 8.80 Hz) 7.60 (d, 2H, *J* = 8.80 Hz), 7.71 (d, 2H, *J* = 8.40 Hz), 8.14 (d, 2H, *J* = 8.40 Hz), 8.24 (d, 2H, *J* = 8.80 Hz).

2.3 Synthesis of monomer

A monomer (2,5-bis-(2,3-dihydrothieno[3,4-b][1,4]dioxyin-5-yl)pyridine) (BEDOT-Pyr) was synthesized based on the method previously reported by Dubois and Reynolds in 2002 [33]. Quantity used in Solution 1: 3,4-ethylene dioxythiophene (EDOT, 1.32 g, 5.57 mmol), *n*-butyl lithium (*n*-BuLi) (16.8 mmol), $ZnCl_2$ (2.27 g, 16.7 mmol), THF (48 mL); in Solution 2: $Pd(PPh_3)_4$ (47.65 g, 0.0412 mmol), 2,5-dibromopyridine, THF (2 mL). Solution 1 and Solution 2 were mixed and reacted for 12 h. Purification with column chromatography (dichloromethane) followed by recrystallization from ethanol obtained 0.90 g (Y = 50 %) of the pure monomer.

2.3 Polymerization

The cholesteric LC electrolyte was prepared by addition of the chiral inducer, TBAP (electrolyte), and the monomer in 6CB (LC solvent). The composition of the constituents of the cholesteric LC electrolytes is summarized in Table 3. The cholesteric LC electrolyte solution was injected between two ITO-coated glass electrodes sandwiching a Teflon sheet (thickness = 0.2 mm) as a spacer. Polymerization was performed with application of constant 4.0 V direct-current voltage applied between the electrodes (Table 3, bottom). During polymerization, the temperature was held at 21.0 ºC in order to maintain the cholesteric LC phase. After 30 min, a thin polymer film had deposited on the anode side of ITO glass electrode. The residual cholesteric LC solution was washed off with hexane to obtain a polymer film.

3. Results and discussions

3.1 Helical sense and helical twisting power

Miscibility testing for determination of the helical sense of TFMHPOBC was performed. Cholesteryl oleyl carbonate with an anticlockwise helical architecture was employed as a standard cholesteric LC. In the miscibility test, no nematic phase was observed on the boundary of the sample with the cholesteryl oleyl carbonate on a glass cell at 45 ºC as shown in Fig. 2. If a standard material and a test sample have the opposite helical sense, the helical twist of the cholesteric LC would unwind, and Schlieren texture of the nematic phase with no helicity would be observed at the boundary of the two compounds. Therefore, this result confirms that TFMHPOBC has an anticlockwise helical architecture at the molecular level. Other compounds employed in this study show the same result as TFMHPOBC in the miscibility test.

The macroscopic helical twisting power (β_M) of these materials was examined by the Grandjean-Cano wedge method [34,35]. The β_M values of the chiral inducers are in the range

of 16.0–23.4 μm^{-1}, indicating that the chiral inducers have high helical twisting power. Furthermore, we obtained helical twisting power (HTP) and molar helical twisting power (MHTP) when compensation for the molecular weight of the materials was calculated as described in the literature [36,37]. HTP and MHTP are estimated by the following formulas,

$$\mathrm{HTP} = (p \cdot c)^{-1},$$
$$\mathrm{MHTP} = \mathrm{HTP} \cdot (M_d/1000),$$
$$\beta_M = (p \cdot c \cdot M_h/M_d)^{-1}.$$

Here, p is the helical pitch, c is the concentration (in wt%) of the chiral inducer, M_h is the molecular weight of the solvent and M_d is the molecular weight of the chiral inducer. The results are summarized in Table 2. Helical twisting power of the materials with the methyl group at the chiral center is larger than that with trifluoromethyl, and the helical twisting power generally increases with a decrease of the flexible terminal alkyl chain length.

3.2 Surface texture

POM and SEM images of the polymer are shown in Fig. 3. The polymer films display a spiral texture (Figs. 3(a,b)) quite similar to that of cholesteric LCs. This result indicates that the polymer transcribed the macroscopic arrangement of the cholesteric LC electrolyte solution during the electrochemical polymerization. Magnified images reveal that the polymer has periodic convex-concave structure and the fingerprint lines consist of lanes of pebble-like structures, as shown in Figs 3(c,d). These images indicate that the polymer fine pebbles grow from the substrate surface via an epitaxial electropolymerization process.

Fig. 4 shows SEM images at 2000 X of polymers prepared by this method containing TFMHPOBC, TFMHPDBC, MHPOBC, and MHPDBC. All of the polymers exhibit fingerprint structure. Distance between fingerprint lines (corresponding to the helical half-pitch of the polymers) vs. helical twisting power of the chiral inducers is plotted in Fig. 5. The helical pitch length of the polymer is inversely proportional to the helical twisting power of the three-ring type chiral inducers. This result indicates that an increase in helical twisting power of the chiral inducer creates a tight-packing helical structure of the matrix chiral LC (cholesteric LC, reaction solvent), and that the resultant polymer synthesized in the cholesteric LC also has tight packing helicity. In other words, helicity of the polymer depends on the helical twisting power of the chiral inducers employed in the polymerization.

The normally observed color of the polymer is deep brown. However, oblique incident white light reveals jewel beetle-like iridescent reflection, as shown in Fig. 6. This is a structural color derived from the periodic convexo-concave stripes of the fingerprint texture. The polymers synthesized in this study are not liquid crystals, but they exhibit interference color due to diffraction via the periodic surface structure produced by the 3-D transcription of cholesteric LC structure in the polymerization process.

3.2 Optical Activity

Fig. 7 shows the CD spectra of the polymer film prepared in the cholesteric LC electrolyte solution containing TFMHPOBC at various applied potentials against an Ag/Ag^+ reference electrode during an electrochemical redox process. The polymer at –1.0 V (reduced state) exhibited a CD signal of – 46 mdeg at 595 nm. The CD intensity (modulus) decreased, accompanied by a red shift in the trough from 595 nm to 640 nm with increase of applied voltage (electrochemical oxidation process). This can be due to the fact that electrochemical

doping of the polymer generates polarons (radical cations) and a new optical absorption band that appears at long wavelengths. Therefore, the CD absorption corresponds to the generation of polarons in oxidation (doping). The signal intensity was restored at
–1.0 V with decrease of applied voltage (electrochemical reduction process). The spectral form is a Davydov split pattern in the CD at the reduced state (at lower applied voltage), indicating that the main chains form π-stacking structures and occasional intermolecular electronic communication between main chains. Furthermore, from the long to short wavelengths in the CD of the polymer at –1.0 V, a change in sign of the signal is observed from negative to positive. This suggests that the chromophores (main chains) are in the left-handed helical sense [38]. The helical sense of the polymer evaluated by the CD corresponds to the helical twisting direction of the cholesteric LC produced by the chiral inducer. The chiral inducer has an anticlockwise helical architecture at the molecular level, as shown in Table 2. Increase of applied voltage allows electrochemical doping of perchlorate ion to the polymer, resulting in an extension of the intermolecular distance between main chains and a decrease of intermolecular interaction due to the intrusion of the ions between helical π-stacked main chains.

Polarons (radical cations) can be generated along the individual main chains. The polarons consist of planer quinoid structures which decrease helical twist of the main chains. Electrochemical oxidation processes (increase of voltage, doping of perchlorate ion) for the polymer decrease the chiroptical activity, accompanied by a decrease of helicity (both helical π-stacking and helical twist of the individual main chains) at the molecular level. This redox (doping-dedoping) cycle is repeatable.

3.3 UV-Vis

Fig. 8 shows the UV absorption of the films synthesized in cholesteric LC. Absorption bands at short wavelengths are due to an optical transition of the monomer repeat unit and at long wavelengths are due to a π–π* transition of the conjugated main chain.

3.4 ORD

Optical rotatory dispersion (ORD) is one of the most interesting physical properties of asymmetric chemical materials. Fig. 9 shows the changes in optical rotatory dispersion for the films prepared in the cholesteric LC electrolyte solution containing TFMHPOBC at – 1.0 V and + 0.5 V vs. Ag/Ag^+. The optical rotation of the polymer can be tuned by the electrochemically applied voltage. Moreover, the threshold voltage is very low. This result confirms that the polymer thus synthesized is electro-chiroptically active.

3.5 Electrochemical characterization

Electrochemical properties of the film prepared in the cholesteric electrolyte solution induced by TFMHPOBC were examined with cyclic voltammetry (CV) at scan rates of 10, 20, 30, 40, 50, 60, 70, 80, 90, and 100 mV/s in 0.1 M TBAP/acetonitrile solution (Fig. 10). The redox switching of the film in the electrolyte solution defines a quasi-reversible redox process with relatively low oxidation potential. Scan rates vs. anodic and cathodic signal currents of the polymer show a linear dependence, as shown in Fig. 11. This result suggests that the electron transfer can be accessed smoothly and rapidly and that the polymer adheres well to the electrode. The electrochemical transfer of electrons to the counter electrode is not diffusion-limited.

4. Conclusions

Chirality and good affinity of the series of rigid chiral compounds with a nematic LC function as chiral inducers for construction of cholesteric LC with helical architecture. Polymerization of the monomer (achiral) in the cholesteric LC prepared with the inducers produces chiroptically active polymer. The chiral inducer does not chemically react with the monomer in the polymerization process; however growth of the polymer is accelerated in the chiral environment produced by the chiral inducer. The polymer film prepared showed a fingerprint texture similar to that of the electrolyte solution, Furthermore, the polymer exhibited consistent CD and selective reflection of light.

The three-ring type chiral compounds change the polymerization environment from achiral (nematic LC) to chiral (cholesteric LC), and the specific environment develops chiral polymer. In other words, the chiral nature of the inducers transfers to the polymer. This electro-optically active function can be applied for new optical modulators. This research explored a new utility of chiral compounds for production of chiroptical polymers.

Acknowledgements

We would like to thank the Chemical Analysis Division of the Research Facility Center for Science and Technology and the Glass Work Shop of the University of Tsukuba.

Techniques

Optical texture observations were carried out using a Nikon ECLIPS LV-100 high-resolution polarizing microscope. The morphology of the polymer film was studied by scanning electron microscopy (SEM) using a Hitachi S-5500. Optical absorption spectra of the polymers were measured using a Jasco V-630 with a quartz cell. Circular dichroism (CD) and optical rotatory dispersion (ORD) measurements were performed with a Jasco J-720. Cyclic voltammetry (CV) was measured with a μAuto Lab III (the Netherlands) at various scan rates between – 0.3 V and +1.0 V vs. an Ag/Ag^{+} reference electrode. Purity of the compound was checked with a Waters 600S high-pressure liquid chromatography (HPLC) system equipped with a GL Science Inertsil ODS-3 column. A custom-made function generator and temperature control stage were used for the electrochemical polymerization.

Chemicals

4-Benzyloxybenzoic acid (1) (Tokyo Kasei), 1,1,1-trifluoro-2-octanol (2) (Aldrich), and 4'-octyloxy-4-biphenylcarboxylic acid (4) (Wako) were used for the synthesis.

References

[1] D. S. K. Mudigonda, J .L. Boehme, I. D. Brotherston, D. L. Meeker, J. P. Ferraris, Chem. Mater.12 (2000) 1508.
[2] S. Bhattacharyya, E. Kymakis, G. A. J. Amaratunga, Chem. Mater. 16 (2004) 4819.
[3] B. N. Boden, K. J. Jardine, A. C. W. Leung, M. J. MacLachlan, Org. Lett. 8 (2006) 1855.
[4] H. Yan, M. Kajita, N. Toshima, Macromol. Mater. Eng. 288 (2003) 578.
[5] K. Ramanathann, M. A. Bangar, M. Yun, W. Chen, N. V. Myung, A. Mulchandani, J. Am. Chem. Soc.127 (2005) 496.
[6] A. Ravikrishnan, P. Sudhakara, P. Kannan, J. Mater. Sci. 45 (2010) 435.
[7] G. F. Malgas, D. E. Motaung, C. J. Arendse, J. Mater. Sci. 47 (2012) 4282.
[8] Z. Wei, J. Xu, J. Hou, W. Zhou, S. Pu, J. Mater. Sci. 41 (2006) 3923.
[9] Y. Coskun, A. Cirpan, L. Toppare, J. Mater. Sci. 42 (2007) 368.
[10] D. K. Bhat, M. S. Kumar, J. Mater. Sci. 42 (2007) 8158.

[11] M. Brittin, G. R. Mitchell, A. S. Vaughan, J. Mater. Sci. 36 (2001) 4911.
[12] M. G. Manjunatha, A. V. Adhikari, A. Pramod, P. K. Hegde, C. S. S. Sandeep, R. Philip, J. Mater. Sci. 44 (2009) 6069.
[13] W. Czerwiński, L. A. Lindén, J. F. Rabek, J. Mater. Sci. 35 (2000) 455.
[14] L. Ke, V. Chellappan, B. Liu, Z. X. Soh, R. H. T. Soh, S. J. Chua, J. Mater. Sci. 43 (2008) 2818.
[15] J. R. de Oliveira, G. M. Silvae, J. Mater. Sci. 43 (2008) 585.
[16] W. J. Feast, R. H. Friend, J. Mater. Sci. 25 (1990) 3796.
[17] Y. Zou, S. Tan, Z. Yuan, Z. Yu, J. Mater. Sci. 40 (2005) 3561.
[18] G. Sönmez, A. Sezai Saraç, J. Mater. Sci. 37 (2002) 4609.
[19] M. Z. Wang, S. B. Feng, X. Y. Zhao, J. Mater. Sci. 41 (2006) 3609.
[20] L. Bonoldi, A. Calabrese, A. Pellegrino, N. Perin, R. Po, S. Spera, A. Tacca, J. Mater. Sci. 46 (2011) 3960.
[21] L. Goris, K. Haenen, M. Nesládek, P. Wagner, D. Vanderzande, L. De Schepper, J. D'haen, L. Lutsen, J. V. Manca, J. Mater. Sci. 40 (2005) 1413.
[22] W. Czerwiński, G. Wrzeszcz, K. Kania, J. F. Rabek, L. A. Lindén, J. Mater. Sci. 35 (2000) 2305.
[23] A. Wei, J. Xu, J. Hou, W. Zhou, S. Pu, J. Mater. Sci. 41 (2006) 3923.
[24] H. Goto, Mater. Chem. Phys. 122 (2010) 69.
[25] H. Yoneyama, K. Kawabata, A. Tsujimoto, H. Goto, Electrochem. Commun., 10, (2008) 965.
[26] T. Tsuruta, S. Inoue, F. Furukawa, J. Macromol. Chem. 84 (1965) 298.
[27] (a) A. D. L. Chandani, T. Hagiwara, Y. Suzuki, Y. Ouchi, H. Takezoe, A. Fukuda, Jpn. J. Appl. Phys. 27 (1988) L729; (b) A. D. L. Chandani, Y. Ouchi, H. Takezoe, A. Fukuda, K. Terashima, K. Furukawa, A. Kishi, Jpn. J. Appl. Phys. 28 (1989) L1261.
[28] H. Hayashi, M. Takemura, K. Kukuchi, Y. Hijikata, H. Orihara, Y. Ishibashi, Jpn. J. Appl. Phys. 31 (1992) 3182.
[29] K. Furukawa, K. Terashima, M. Ichihashi, S. Saitoh, K. Miyazawa, T. Inukai, Ferroelectrics 85 (1988) 451.
[30] H. Hayashi, M. Takemura, Y. Yamada, K. Kikuchi, K. Takigawa, M. Inata, Y. Hijikata, K. Ezaka, H. Shindo, H. Orihara, Y. Ishibashi, Jpn. J. Appl. Phys. 33 (1994) 5494.
[31] H. Hayashi, M. Takemura, K. Kikuchi, K. Takigawa, M. Inata, Y. Hijikata, K. Ezaka, H. Shindo, H. Orihara, Y. Ishibashi, Jpn. J. Appl. Phys. 34 (1995) 5438.
[32] T. Kitazume, T. Yamazaki, H. Iwatsubo, (1991) US Pat ,5047346A 19910910.
[33] C. J. Dubois, J. R. Reynolds, Adv. Mater. 14 (2002) 1844.
[34] M. Wilson, D. J. Earl, J. Mater. Chem. 11 (2001) 2672.
[35] Y. Aoki, K. Matsushima, T. Taruoka, T. Hirose, H. Nohira, Mol. Cryst. Liq. Cryst. 398 (2003) 189.
[36] Y. Aoki, S. Nomoto, T. Hirose, H. Nohira, Mol. Cryst. Liq. Cryst. 346 (2000) 35.
[37] Y. Aoki, H. Nohira, Liq. Cryst. 18 (1995) 197.
[38] H. W. Liu, K. Nakanishi, J. Am. Chem. Soc. 103 (1981) 5591.

Table 1 Chemical structures of chiral inducers.

Abbreviation	Molecular Structure
TFMHPOBC	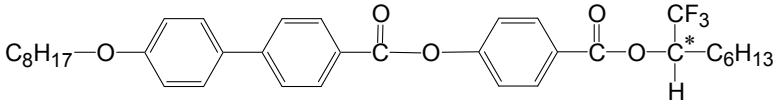
TFMHPDBC	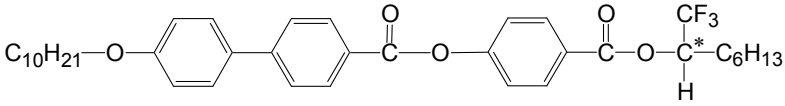
MHPOBC	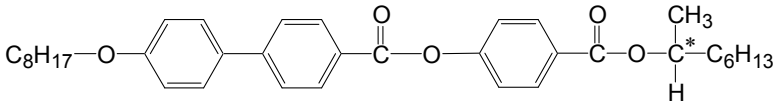
MHPDBC	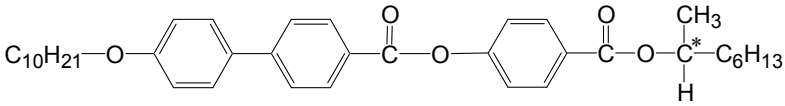

* = stereogenic center

Table 2 Helical twisting power and helical sense of chiral inducers.

Chiral inducer	LC solvent	HTP[b] (μm^{-1})[b]	MHTP[c] ($\mu m^{-1} mol^{-1} kg$)	β_M[d] (μm^{-1})	H[e]
TFMHPOBC	6CB[a]	8.07	4.95	18.8	Anti[f]
TFMHPDBC	6CB[a]	6.58	4.22	16.0	Anti[f]
MHPOBC	6CB[a]	11.01	6.15	23.4	Anti[f]
MHPDBC	6CB[a]	10.46	6.14	23.3	Anti[f]

[a]6CB (4-cyano-4'-*n*-hexyl biphenyl): 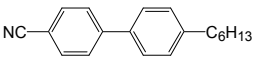

[b]HTP (helical twisting power) = $(p \cdot c)^{-1}$, p = helical pitch; c = weight conc. of the chiral inducer
[c]MHTP (molar helical twisting power) = HTP$\cdot M_d \cdot 10^{-3}$, M_d = molecular weight of the chiral inducer, M_h = molecular weight of the solvent.
[d]$\beta_M = (p \cdot c \cdot M_h / M_d)^{-1}$
[e]Helical sense
[f]Anticlockwise direction

Table 3 Composition of cholesteric electrolyte solutions containing monomer.

Chiral inducer (mg, μM)[a]	Solvent (mg, μM) [a]	Electrolyte (supporting salt) (mg, μM)[a]	Monomer[b] (mg, μM)[a]
TFMHPOBC (9.25, 15.1)	6CB[b] (120.1, 456)	TBAP[c] (0.50, 1.5)	BEDOT-Pyr[d] (1.89, 5.26)
TFMHPDBC (9.69, 15.0)	6CB[b] (123.3, 469)	TBAP[c] (0.54, 1.6)	BEDOT-Pyr[d] (2.00, 5.56)
MHPOBC (8.27/14.8)	6CB[b] (117.4, 446)	TBAP[c] (0.53, 1.6)	BEDOT-Pyr[d] (2.06, 5.73)
MHPDBC (8.80, 15.0)	6CB[b] (117.5, 447)	TBAP[c] (0.55, 1.6)	BEDOT-Pyr[d] (2.00, 5.56)

[a]Sample weight and mole amount

[b]6CB (4-cyano-4'-*n*-hexyl biphenyl): 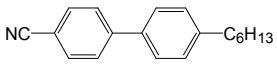

[c]TBAP (tetrabutyl ammonium perchlorate): $[CH_3(CH_2)_3]_4NClO_4$

[d]BEDOT-Pyr 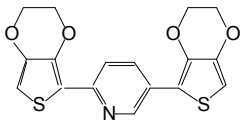

Polymerization:
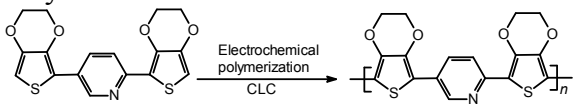

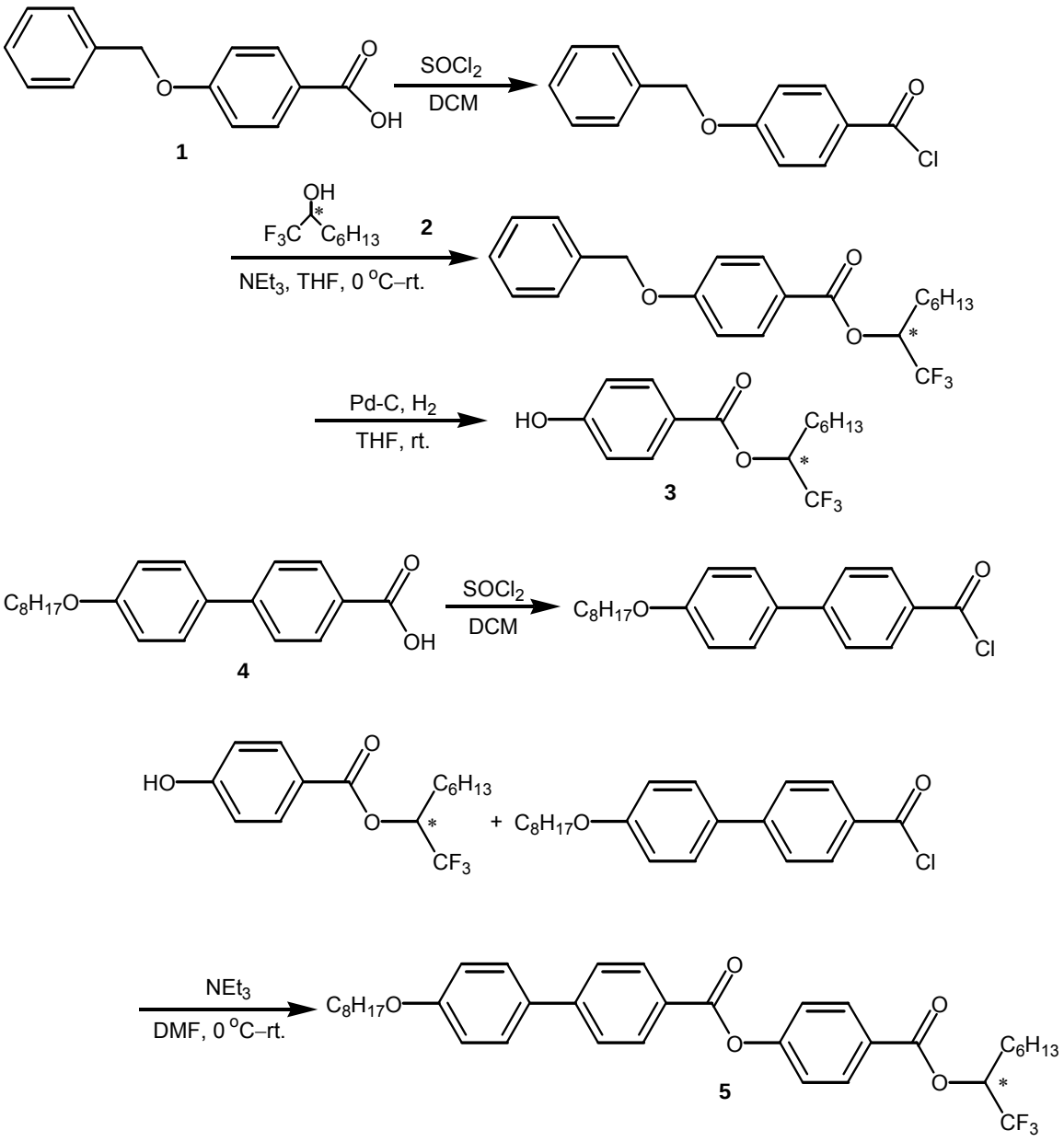

Scheme 1. Synthetic route of 4-(1-trifluoromethyl heptyloxy carbonyl) phenyl-4'-octyloxy biphenyl-4-carboxylate (TFMHPOBC). DCM = dichloromethane, THF = tetrahydrofuran, NEt_3 = triethylamine, DMF = dimethyl formamide.

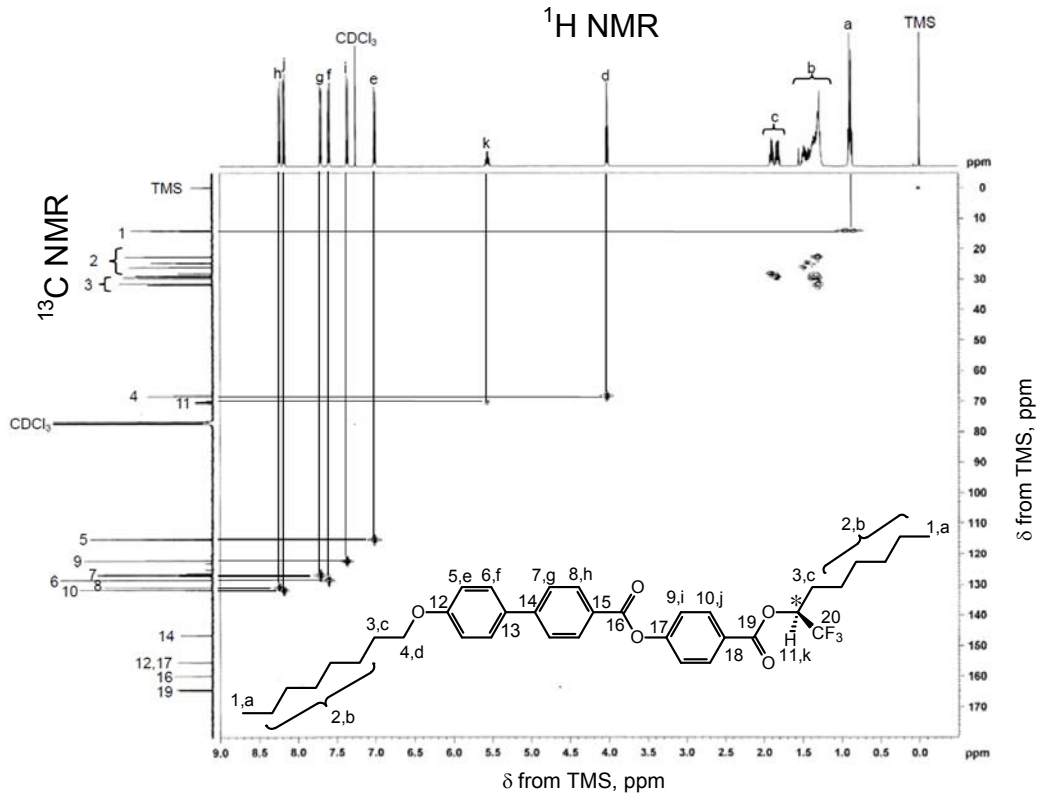

Fig. 1 2D-NMR (HMQC, Hetero-nuclear Multiple Quantum Coherence) analysis result of TFMHPOBC.

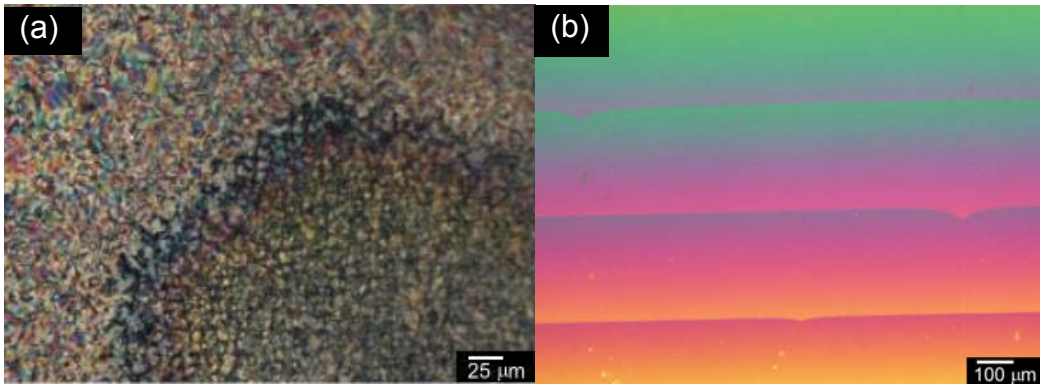

Fig. 2 (a) Polarizing optical microscopy (POM) images of miscibility test. (b) An example of Cano-wedge cell (TFMHPOBC in 6CB).

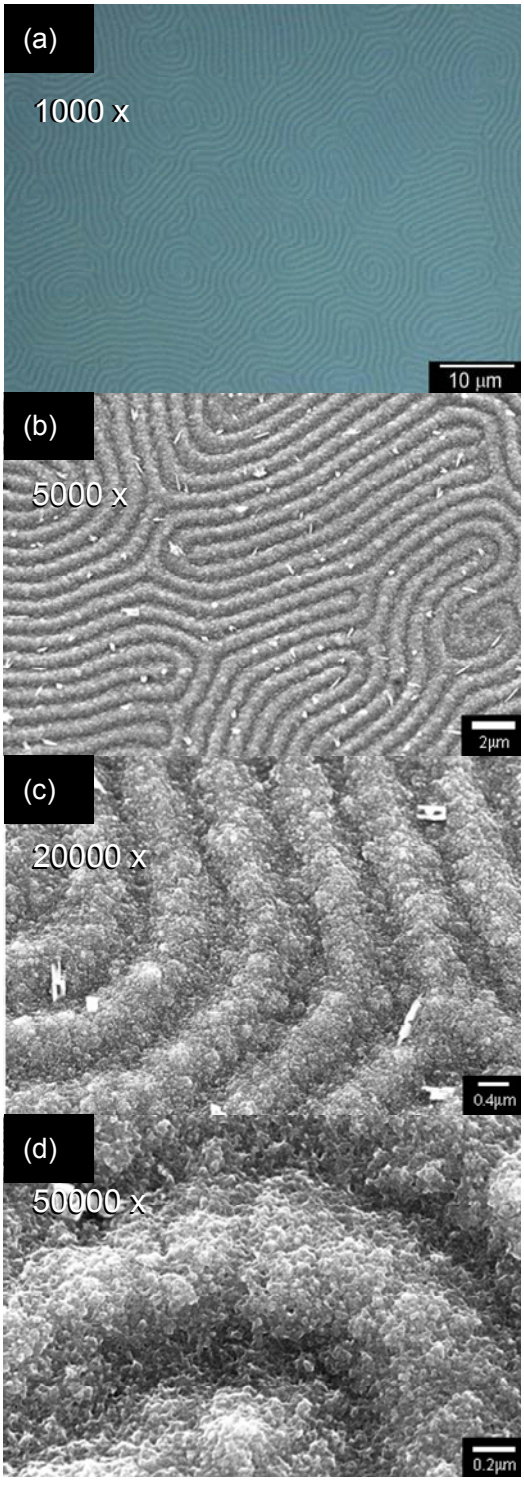

Fig. 3 POM and SEM images of polymer prepared by the electrochemical method in cholesteric LC induced by TFMHPOBC. (a) POM image, magnification 1000 ×. (b)–(d) SEM images taken from a direction oriented 20 ° from the surface.

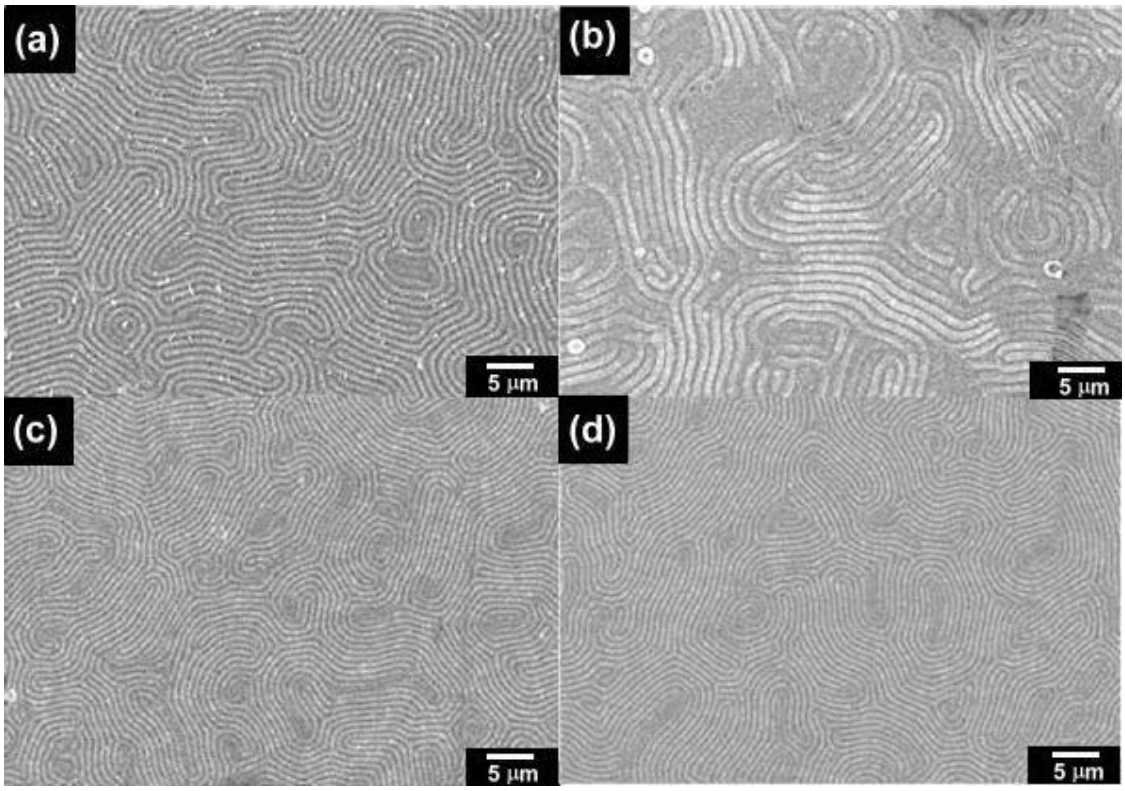

Fig. 4 SEM images of polymers prepared by the electrochemical method in cholesteric LC solution at 2000 ×. (a) Polymer prepared in cholesteric LC solution induced by TFMHPOBC. (b) Polymer prepared in cholesteric LC solution induced by TFMHPDBC. (c) Polymer prepared in cholesteric LC solution induced by MHPOBC. (d) Polymer prepared in cholesteric LC solution induced by MDPHDBC.

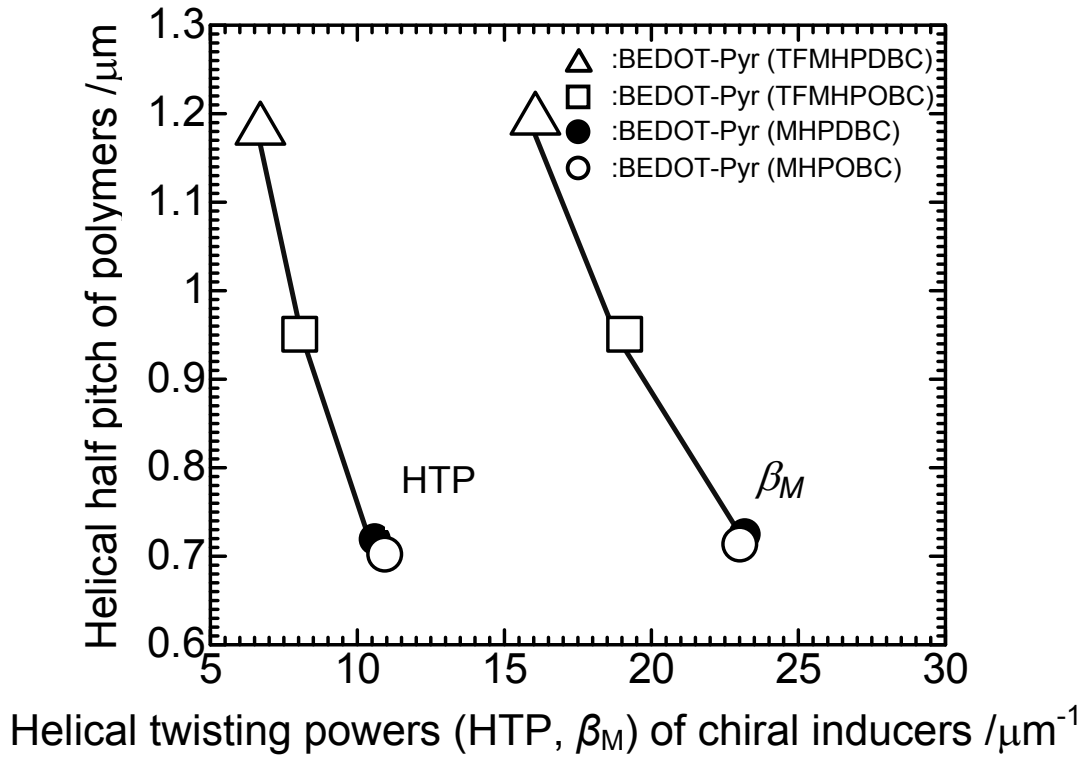

Fig. 5 Helical half-pitch of the resultant polymers prepared in cholesteric LC solutions vs. helical twisting powers (HTP, β_M) of the chiral inducers.

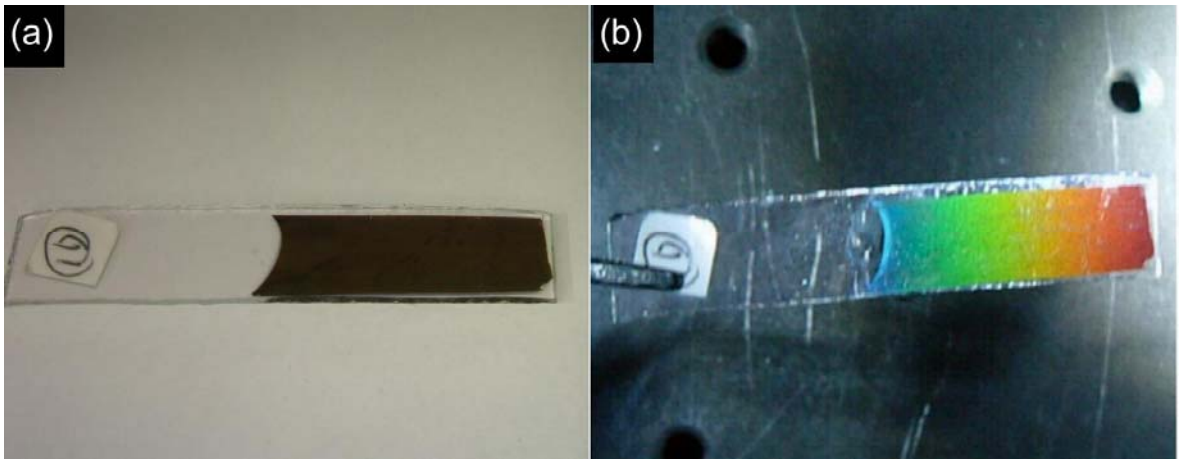

Fig. 6 Visible images of the polymer prepared in cholesteric LC solution induced by TFMHPOBC. (a) Natural appearance. (b) Multi-color reflection upon irradiation of oblique incident white light.

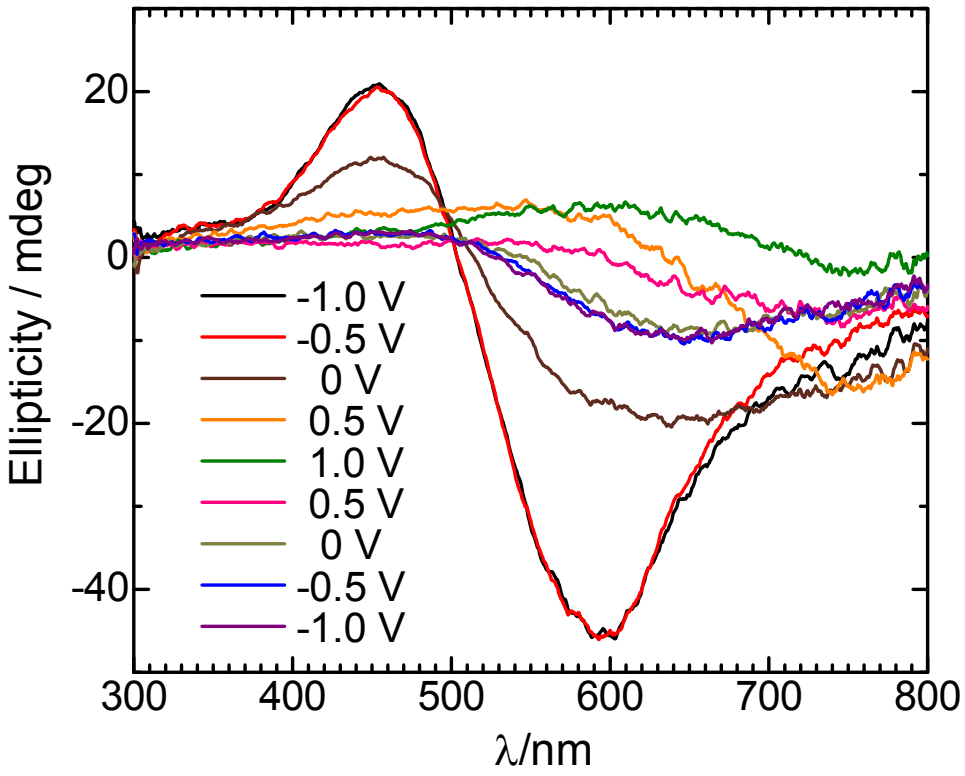

Fig. 7 CD spectra of the film prepared from cholesteric LC solution induced by TFMHPOBC.

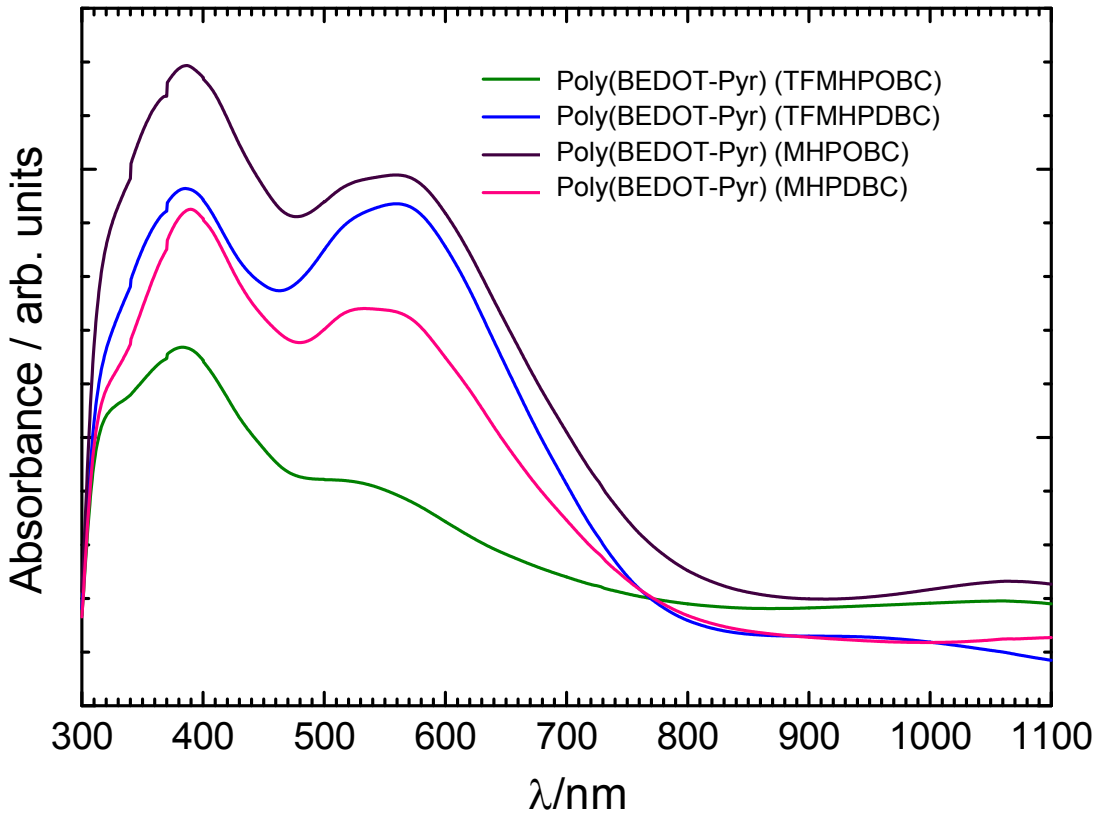

Fig. 8 UV spectra of the films prepared from the cholesteric LC electrolyte induced by the series of the three-ring type chiral compounds.

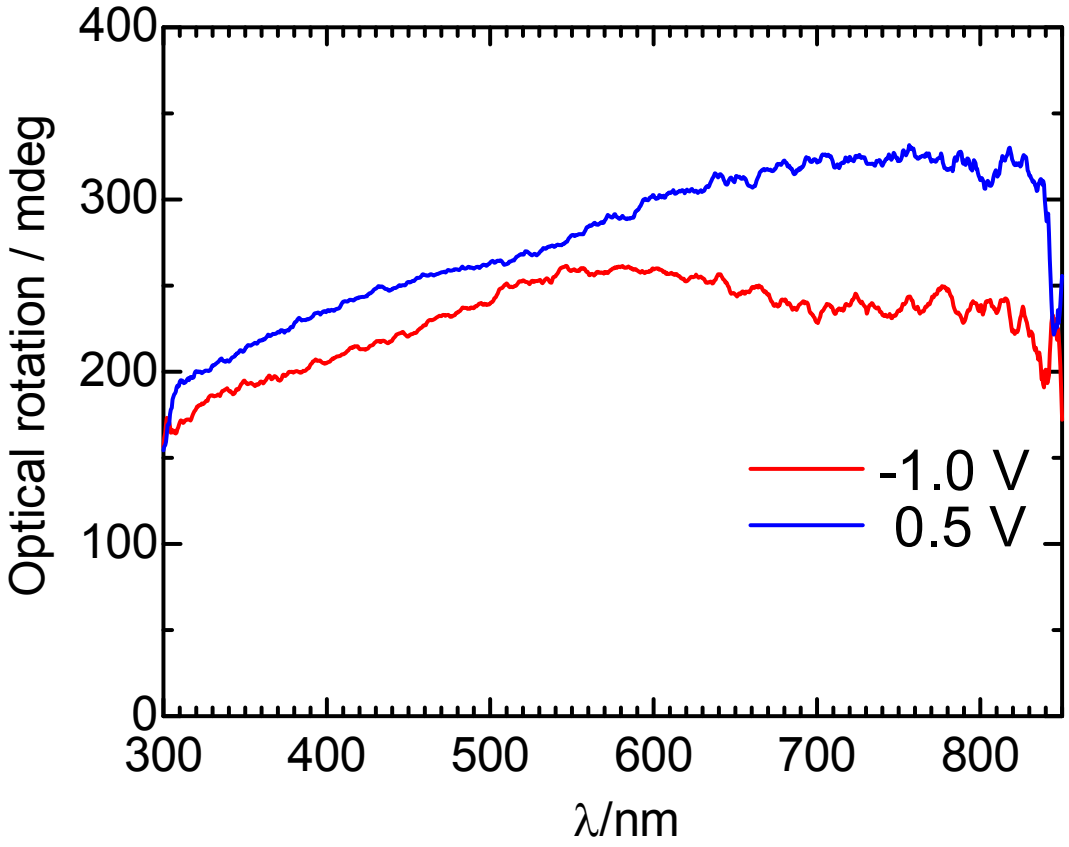

Fig. 9 Optical rotatorory dispersion (ORD) spectra of the film prepared from cholesteric LC solution induced by TFMHPOBC.

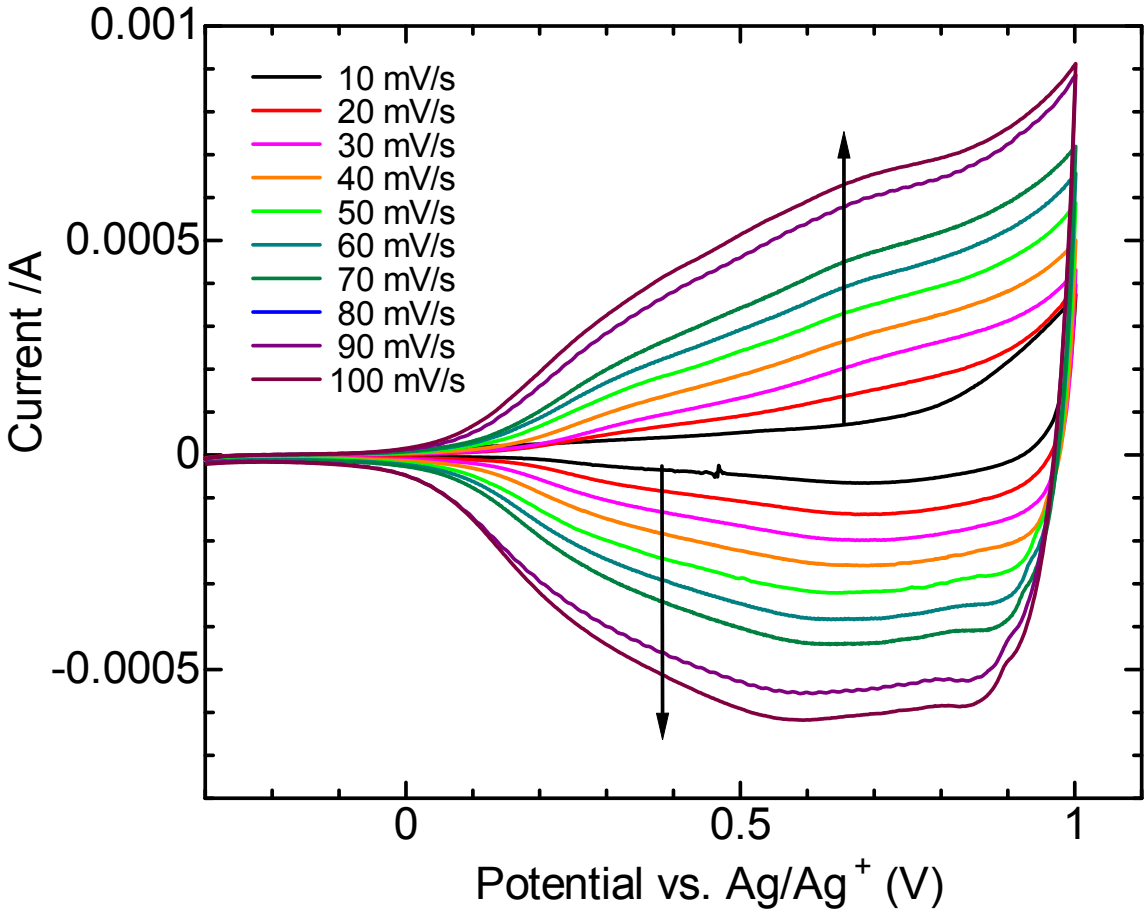

Fig. 10 Cyclic voltammetry (CV) measurements of the film prepared in cholesteric LC electrolyte solution induced by TFMHPOBC at various scan rates.

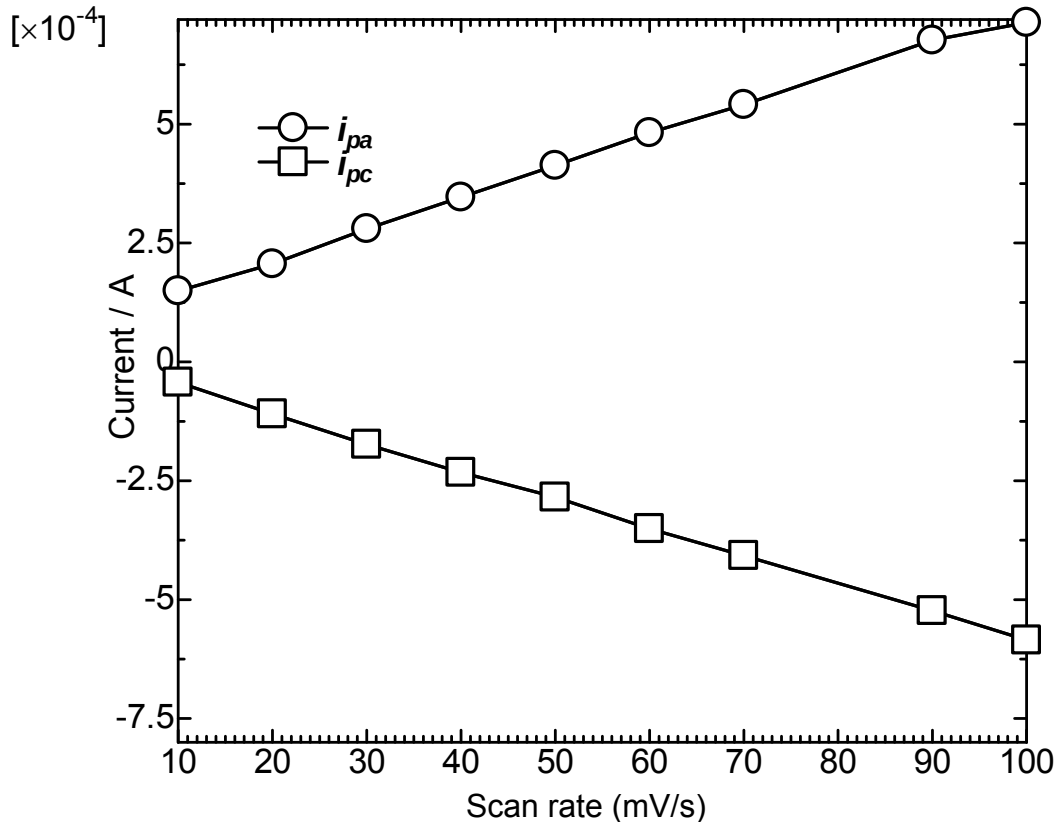

Fig. 11 Current vs. scan rate plots obtained with CV measurements for the polymer film prepared in cholesteric LC electrolyte solution induced by TFMHPOBC at various scan rates. The i_{pa} and i_{pc} reveal anodic peak current, cathodic peak current respectively.

Supplementary data for:

Helical Twisting Power of Three-ring Chiral Materials, and Their Polymerization in Chiral Liquid Crystals

Hitoshi Hayashi,[1,2] Aohan Wang,[2] Kohsuke Kawabata,[2] Hiromasa Goto[2,*]

[1]Advanced Research, Research Laboratories, DENSO CORPORATION, 500-1, Minamiyama, Komenoki-cho, Nisshin, Aichi 470-0111, Japan.

[2] Division of Materials Science, Faculty of Pure and Applied Sciences, University of Tsukuba, Tsukuba, Ibaraki 305-8573, Japan

Corresponding to H. Goto, e-mail: gotoh@ims.tsukuba.ac.jp

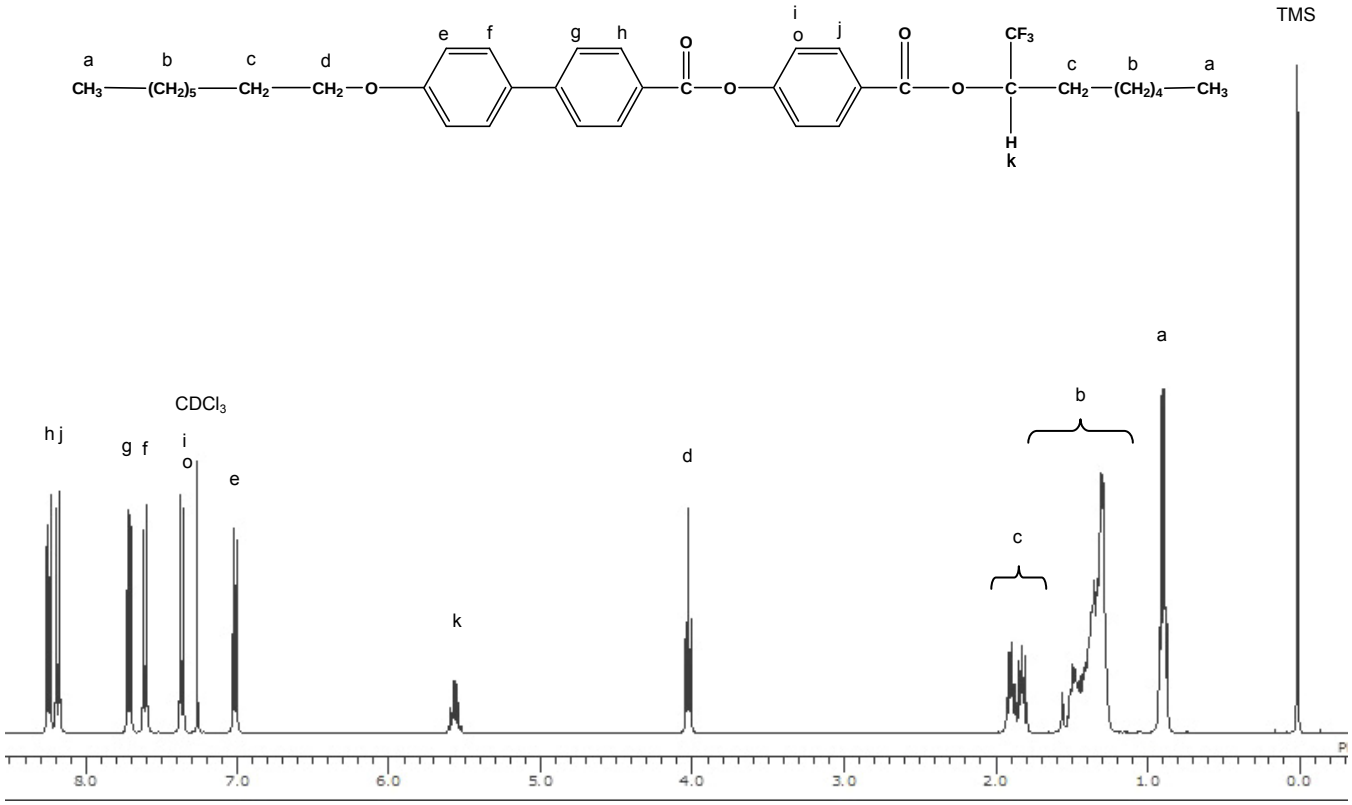

Figure S1. ^{1}H NMR of TFMHPOBC.

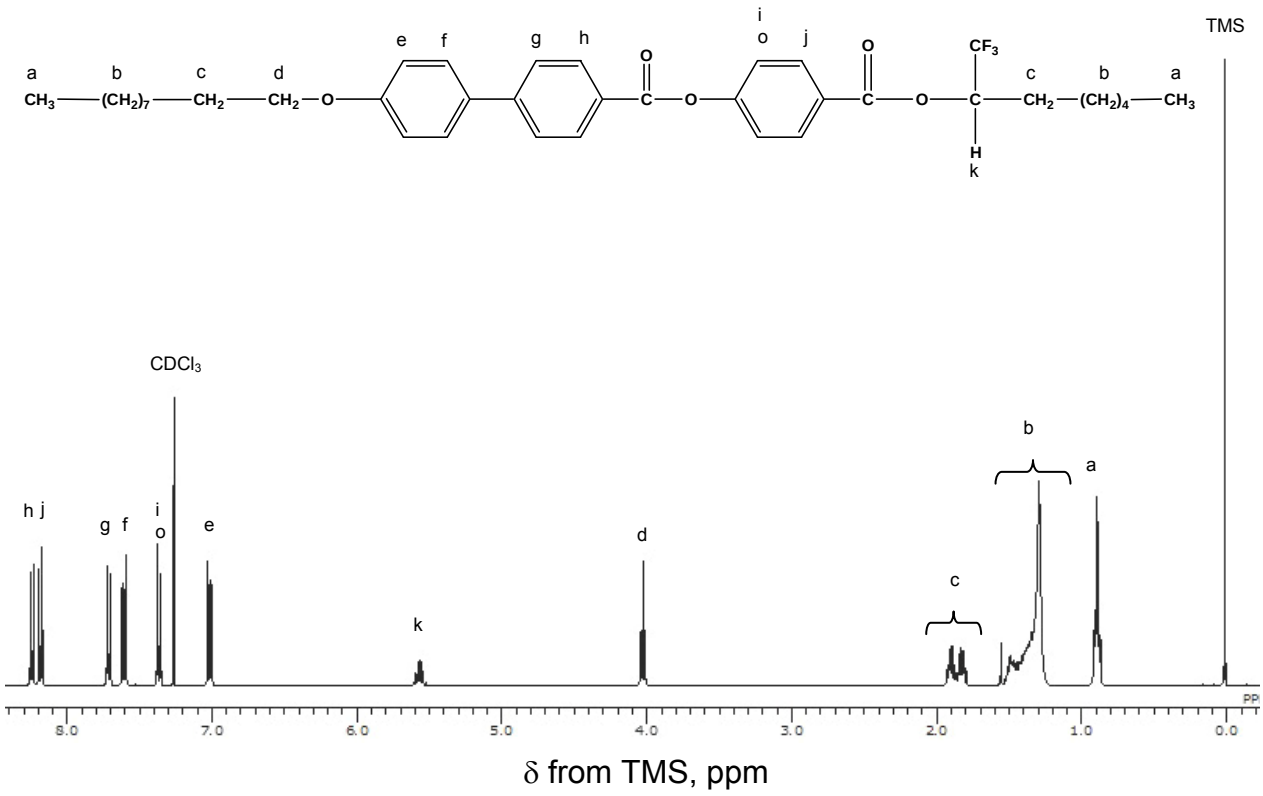

Figure S2. ^{1}H NMR of TFMHPDBC.

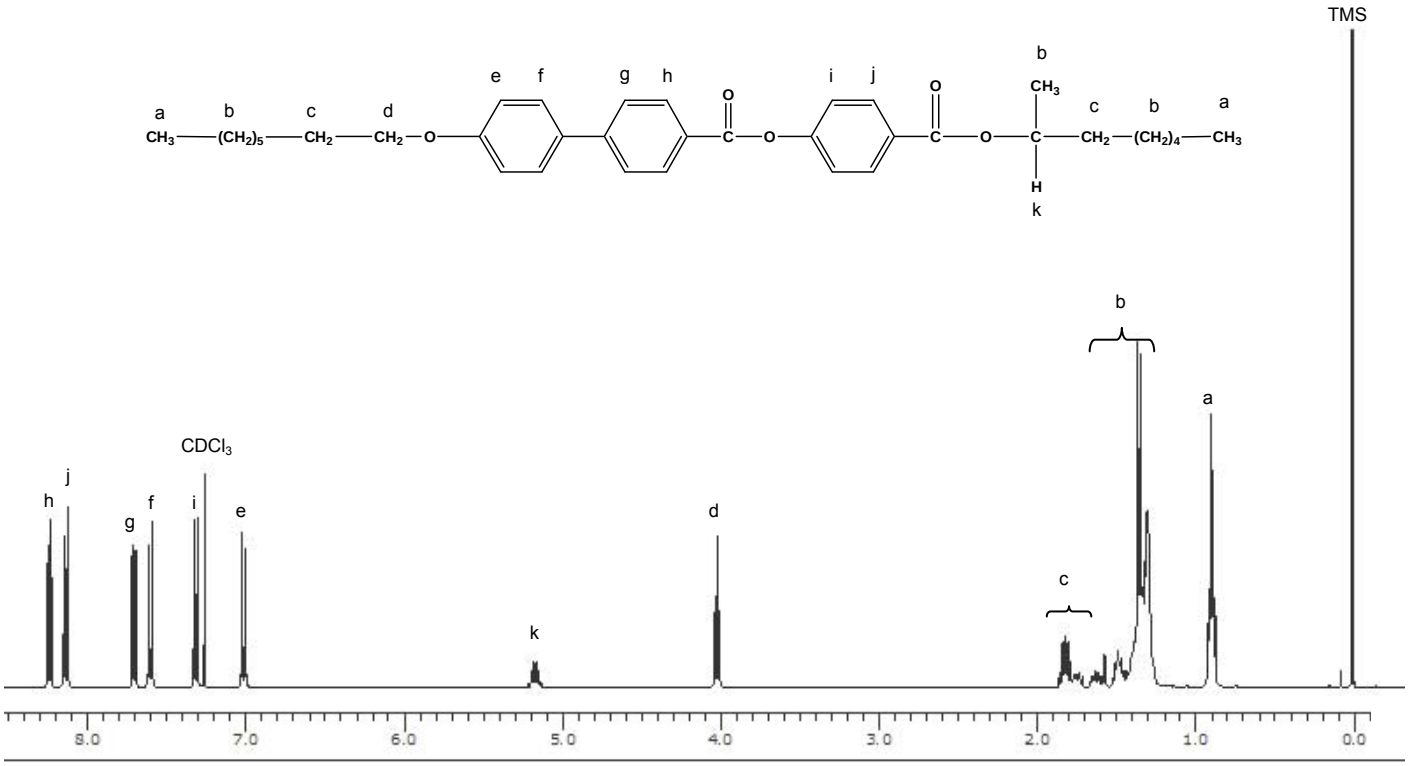

Figure S3. ^{1}H NMR of MHPOBC.

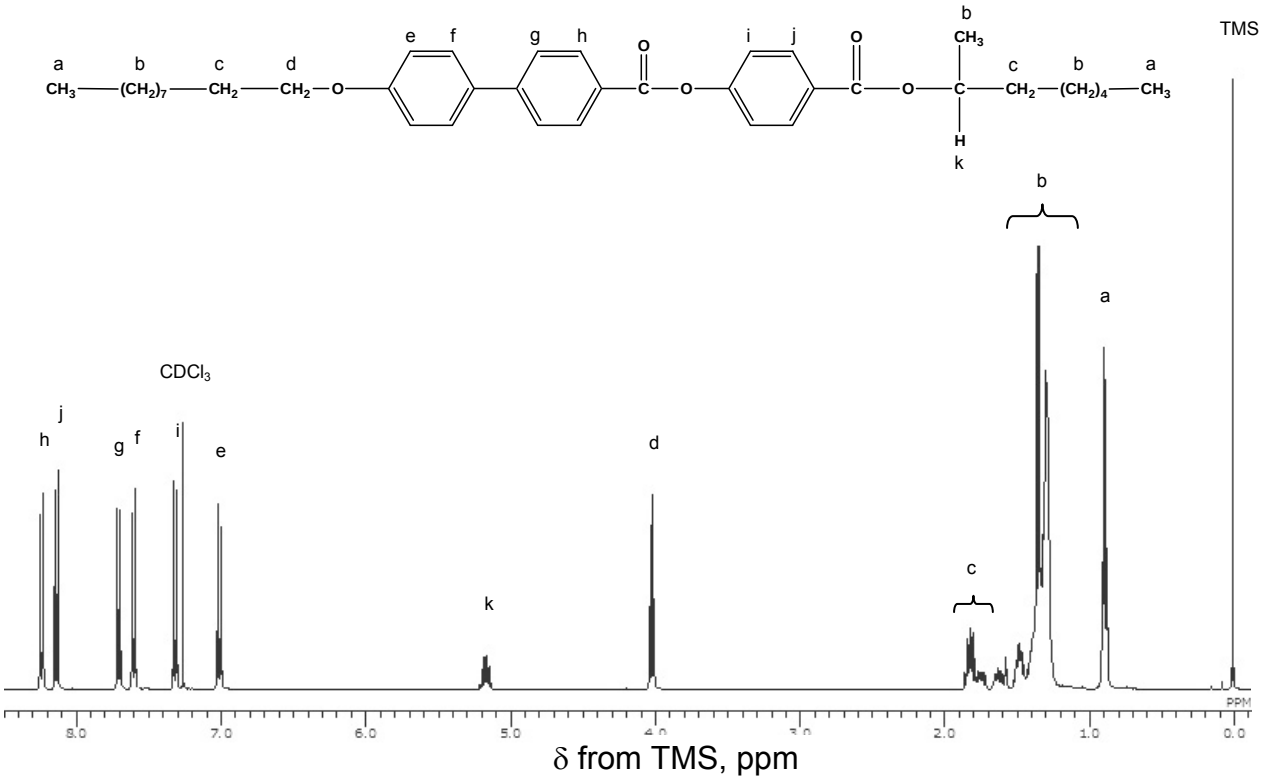

Figure S4. ^{1}H NMR of MHPDBC.

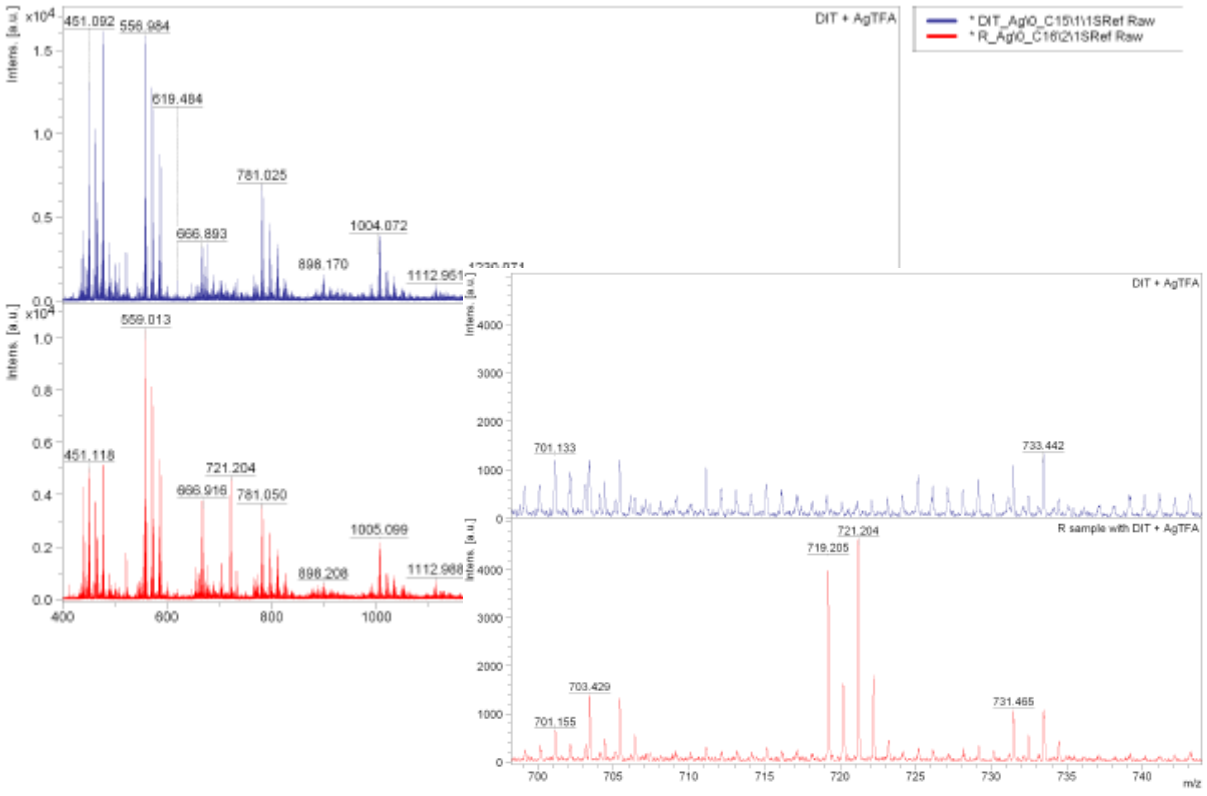

Figure S5. MS spectrum of TFMHPOBC

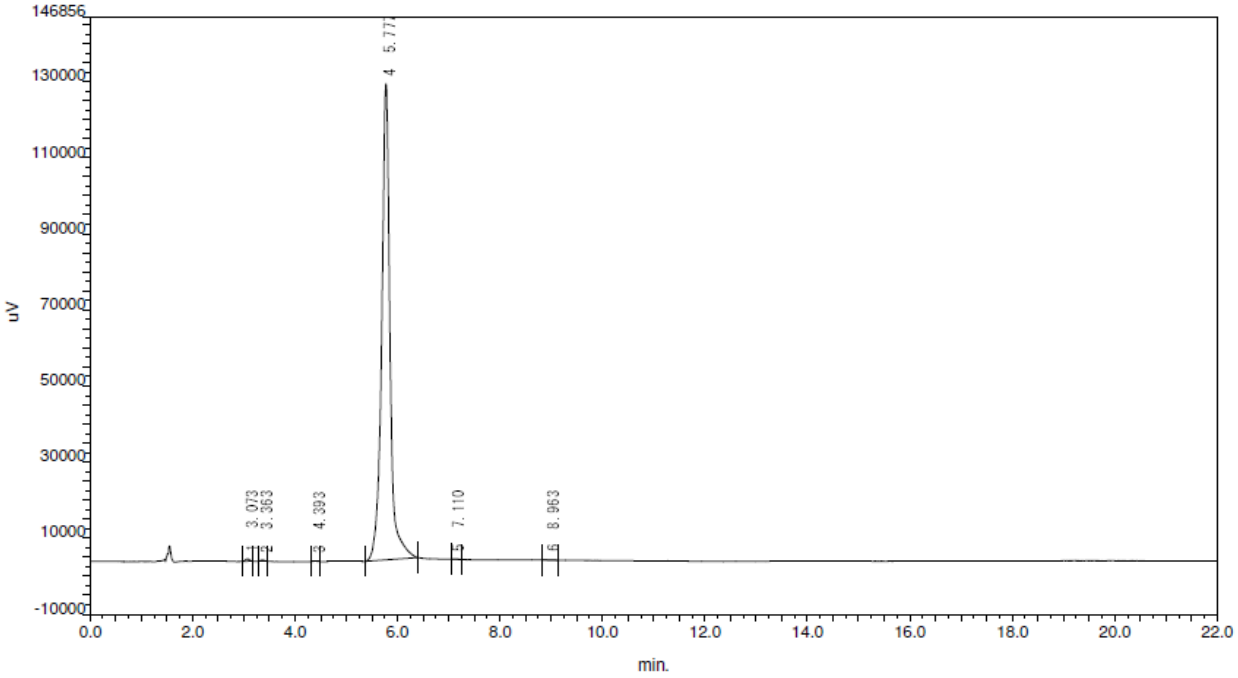

Figure S6. High pressure liquid chromatography (HPLC) chart of TFMHPOBC